Journal of Applied Mechanics Vol.8, pp.179-187 (August 2005) JSCE

Free Vibration Analysis of Rectangular Plates with Multiple Point Supports

多点支持された長方形板の自由振動の一解析法

M. Huang [*1], X.Q. Ma [*2], T.Sakiyama [*3], H. Matsuda [*4], C. Morita [*5]
黄 美, 馬秀琴, 崎山 毅, 松田 浩, 森田 千尋

[*1]Member of JSCE, Dr.of Eng., Res. Assoc., Dept.of Struct. Eng. Nagasaki Univ. (852-8521, Nagasaki)
[*2]Assoc.Prof., Hebei Univ. of Tech., P.R.China
[*3]Member of JSCE, Dr.of Eng., Prof., Dept.of Struct. Eng. Nagasaki Univ. (852-8521, Nagasaki)
[*4]Member of JSCE, Dr.of Eng., Prof., Dept.of Struct. Eng. Nagasaki Univ. (852-8521, Nagasaki)
[*5]Member of JSCE, Dr.of Eng., Assoc.Prof., Dept.of Struct. Eng. Nagasaki Univ. (852-8521, Nagasaki)

Free vibration problem of rectangular plates with multiple point supports is analyzed by a discrete method. The concentrated loads with Dirac's delta functions are used to simulate the point supports which limit the displacements of the plate but don't offer constraint on the slopes. The fundamental differential equations are established for the bending problem of the plate with point supports. The solution of these equations is obtained by transforming these differential equations into integral equations and using numerical integration. Green function which is the solution of deflection is used to obtain the characteristic equation of the free vibration. The effects of the number and positions of point supports, the boundary condition and the aspect ratio on the frequencies are considered. By comparing the numerical results obtained by the present method with those previously published, the efficiency and accuracy of the present method are investigated.

Key Words : *discrete method, multiple point supports, Green function, vibration*

1. Introduction

The free vibration analysis of the rectangular plates with point supports has received considerable attention during the past decades. According to the positions of the point supports, two kinds of the plates with point supports have been studied. One is the plate with point supports along the edges. Another is the plate with interior point supports. Bapat, Venkatramani and Suryanarayan [1,2] investigated the free vibration of rectangular plates with symmetrical and asymmetrical point supports along the edges, respectively. The flexibility function approach and the impulse function approach were used to simulate the point supports. By using these two approaches, some results were obtained for plates having two opposite edges simply supported and two other edges free with simply or clamped mid-point supports. A comparison of these two methods was also given and the advantage of the flexibility function method was shown. By using the same methods, they [3] also studied the free vibration of rectangular plates with interior point supports. The plates with two opposite edges simply supported and classical boundary conditions on the other edges were studied. One or more interior point supports existed along a line perpendicular to the simply supported edges. By dividing the plate into two subplates and satisfying the continuity conditions along the partition line and the compatibility at the point support, a set of equations were obtained. From the set of equations and the equivalent equations, the coefficient matrix was obtained and its determinant was set to be zero to obtain the characteristic equation. The effects of the boundary condition, aspect ratio and the positions of the point supports were considered. The free vibration problems of the rectangular plates with point supports were also studied in references [4–7]. Recently, Zhao, Wei and Xiang [8] used discrete singular convolution method to solve plate

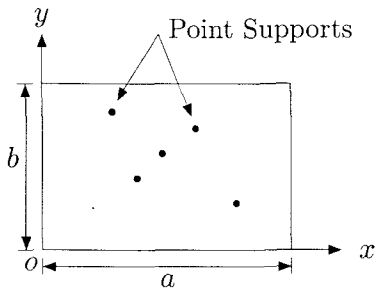

Fig. 1 A rectangular plate with point supports.

vibration with irregular internal supports. Some results were obtained for plates with a pattern of double rhombuses or randomly distributed points support points. The discrete singular convolution method is very powerful method to handling the problems aforementioned.

In this paper, a discrete method [10–13] is extended for analyzing the free vibration of rectangular plates with multiple point supports. The fundamental differential equations of a plate with point supports involving Dirac's delta functions are established and satisfied exactly throughout the whole plate. By transforming these equations into integral equations and using numerical integration, the solutions are obtained at the discrete points. The Green function, which is the solution for deflection, is used to obtain the characteristic equation of the free vibration. The present method is a general method. It can be used to analyze the free vibration of rectangular plates with multiple point supports along the edges or interior point supports, various aspect ratio and general boundary conditions. The purpose of the paper is (1) to investigate the efficiency and accuracy of the present method for the rectangular plates with point supports by comparing the present results with those reported early, and (2) to investigate the effect of the number and positions of point supports on the frequency parameter of rectangular plates.

2. Fundamental Differential Equations

Consider a rectangular plate with multiple point supports as shown in Figure 1. The length, width, thickness and density of the plate is expressed as a, b, h and ρ, respectively. An xyz coordinate system is used in the present study with its $x-y$ plane contained in middle plane of the rectangular plate, the $z-$axis perpendicular to the middle plane of the plate and the origin at one of the corners of the plate.

In this paper, the concentrated loads with Dirac's delta functions are used to simulate the point supports which limit the displacements of the plate but don't offer constraint on the slopes.

The fundamental differential equations of the plate having a concentrated load $\overline{P}$ at a point (x_q, y_r) and the point support $\overline{P}_{cd}$ at each discrete point (x_c, y_d) are as follows:

$$\begin{aligned}
&\frac{\partial Q_x}{\partial x}+\frac{\partial Q_y}{\partial y}+\overline{P}\delta(x-x_q)\delta(y-y_r)\\
&+\sum_{c=0}^{m}\sum_{d=0}^{n}\overline{P}_{cd}\delta(x-x_c)\delta(y-y_d)=0,\\
&\frac{\partial M_{xy}}{\partial x}+\frac{\partial M_y}{\partial y}-Q_y=0,\\
&\frac{\partial M_x}{\partial x}+\frac{\partial M_{xy}}{\partial y}-Q_x=0,\\
&\frac{\partial \theta_x}{\partial x}+\nu\frac{\partial \theta_y}{\partial y}=\frac{M_x}{D},\\
&\frac{\partial \theta_y}{\partial y}+\nu\frac{\partial \theta_x}{\partial x}=\frac{M_y}{D},\\
&\frac{\partial \theta_x}{\partial y}+\frac{\partial \theta_y}{\partial x}=\frac{2}{(1-\nu)}\frac{M_{xy}}{D},\\
&\frac{\partial w}{\partial x}+\theta_x=\frac{Q_x}{\kappa Gh},\\
&\frac{\partial w}{\partial y}+\theta_y=\frac{Q_y}{\kappa Gh},
\end{aligned}\tag{1}$$

where Q_x, Q_y are the shearing forces, M_{xy} the twisting moment, M_x, M_y the bending moments, θ_x, θ_y the rotations of the x- and y-axes, w the deflection, $D = Eh^3/(12(1-\nu^2))$ the bending rigidity, E, G modulus, shear modulus of elasticity, respectively, ν Poisson's ratio, $\kappa = 5/6$ is the shear correction factor, $\delta(x-x_q)$, $\delta(x-x_r)$, $\delta(x-x_c)$, $\delta(x-x_d)$ Dirac's delta functions.

By introducing the non-dimensional expressions,

$$[X_1, X_2] = \frac{a^2}{D_0(1-\nu^2)}[Q_y, Q_x],$$

$$[X_3, X_4, X_5] = \frac{a}{D_0(1-\nu^2)}[M_{xy}, M_y, M_x],$$

$$[X_6, X_7, X_8] = [\theta_y, \theta_x, w/a],$$

the equation (1) is rewritten as the following non-dimensional forms:

$$\begin{aligned}
&\mu\frac{\partial X_2}{\partial \eta}+\frac{\partial X_1}{\partial \zeta}+P\delta(\eta-\eta_q)\delta(\zeta-\zeta_r)\\
&+\sum_{c=0}^{m}\sum_{d=0}^{n}P_{cd}\delta(\eta-\eta_c)\delta(\zeta-\zeta_d)=0,\\
&\mu\frac{\partial X_3}{\partial \eta}+\frac{\partial X_4}{\partial \zeta}-\mu X_1=0,
\end{aligned}$$

$$\mu\frac{\partial X_5}{\partial \eta}+\frac{\partial X_3}{\partial \zeta}-\mu X_2=0,$$
$$\mu\frac{\partial X_7}{\partial \eta}+\nu\frac{\partial X_6}{\partial \zeta}-IX_5=0,$$
$$\nu\mu\frac{\partial X_7}{\partial \eta}+\frac{\partial X_6}{\partial \zeta}-IX_4=0,$$
$$\mu\frac{\partial X_6}{\partial \eta}+\frac{\partial X_7}{\partial \zeta}-JX_3=0,$$
$$\frac{\partial X_8}{\partial \eta}+X_7-HX_2=0,$$
$$\frac{\partial X_8}{\partial \zeta}+\mu X_6-\mu HX_1=0, \qquad (2)$$

where $\mu = b/a$; $I = \mu(1-\nu^2)(h_0/h)^3$; $J = 2\mu(1+\nu)(h_0/h)^3$; $H = ((1+\nu)/5)(h_0/a)^2(h_0/h)$; $P = \overline{P}a/(D_0(1-\nu^2))$; $P_{cd} = \overline{P}_{cd}a/(D_0(1-\nu^2))$; $D_0 = Eh_0^3/(12(1-\nu^2))$ is the standard bending rigidity; h_0 the standard thickness of the plate; $\delta(\eta-\eta_q)$, $\delta(\zeta-\zeta_r)$, $\delta(\eta-\eta_c)$ and $\delta(\zeta-\zeta_d)$ Dirac's delta functions.

For the plates with uniform thickness, $D = D_0$ and $h = h_0$.

The equation (2) can also be expressed as the following simple form.

$$\sum_{s=1}^{8}\left\{F_{1ts}\frac{\partial X_s}{\partial \zeta}+F_{2ts}\frac{\partial X_s}{\partial \eta}+F_{3ts}X_s\right\}$$
$$+P\delta(\eta-\eta_q)\delta(\zeta-\zeta_r)\delta_{1t}$$
$$+\sum_{c=0}^{m}\sum_{d=0}^{n}P_{cd}\delta(\eta-\eta_c)\delta(\zeta-\zeta_d)\delta_{1t}=0,$$
$$(t=1\sim 8), \qquad (3)$$

where $t = 1 \sim 8$; δ_{1t} is Kronecker's delta; $F_{111} = F_{124} = F_{133} = F_{156} = F_{167} = F_{188} = 1$; $F_{146} = \nu$; $F_{212} = F_{223} = F_{235} = F_{247} = F_{266} = \mu$; $F_{257} = \mu\nu$; $F_{278} = 1$; $F_{321} = F_{332} = -\mu$; $F_{345} = F_{354} = -I$; $F_{363} = -J$; $F_{372} = -H$; $F_{377} = 1$; $F_{381} = -\mu H$; $F_{386} = \mu$; other$F_{kts} = 0$.

3. Discrete Green Function

By dividing a square plate vertically into m equal-length parts and horizontally into n equal-length parts as shown in Figure 2, the plate can be considered as a group of discrete points which are the intersections of the $(m+1)$-vertical and $(n+1)$-horizontal dividing lines. To describe the present method conveniently, the rectangular area, $0 \le \eta \le \eta_i$, $0 \le \zeta \le \zeta_j$, corresponding to the arbitrary intersection (i,j) as shown in Figure 2 is denoted as the area $[i,j]$, the intersection (i,j) denoted by ◯ is called the main point of the area $[i,j]$, the intersections denoted by ○ are called the inner dependent points of the area, and the intersections denoted by • are called the boundary dependent points of the area.

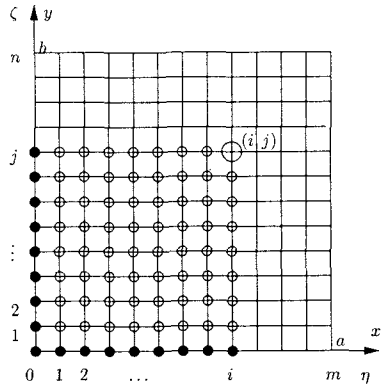

Fig. 2 Discrete points on a rectangular plate.

By integrating the equation (3) over the area $[i,j]$, the following integral equation is obtained:

$$\sum_{s=1}^{8}\left\{F_{1ts}\int_0^{\eta_i}[X_s(\eta,\zeta_j)-X_s(\eta,0)]d\eta\right.$$
$$+F_{2ts}\int_0^{\zeta_j}[X_s(\eta_i,\zeta)-X_s(0,\zeta)]d\zeta$$
$$\left.+F_{3ts}\int_0^{\eta_i}\int_0^{\zeta_j}X_s(\eta,\zeta)d\eta d\zeta\right\}$$
$$+Pu(\eta-\eta_q)u(\zeta-\zeta_r)\delta_{1t}$$
$$+\sum_{c=0}^{m}\sum_{d=0}^{n}P_{cd}u(\eta-\eta_c)u(\zeta-\zeta_d)\delta_{1t}=0, \qquad (4)$$

where $u(\eta-\eta_q)$, $u(\zeta-\zeta_r)$, $u(\eta-\eta_c)$ and $u(\zeta-\zeta_d)$ are the unit step functions.

Next, by applying the numerical integration method, the simultaneous equation for the unknown quantities $X_{sij} = X_s(\eta_i,\zeta_j)$ at the main point (i,j) of the area $[i,j]$ is obtained as follows:

$$\sum_{s=1}^{8}\left\{F_{1ts}\sum_{k=0}^{i}\beta_{ik}(X_{skj}-X_{sk0})\right.$$
$$+F_{2ts}\sum_{l=0}^{j}\beta_{jl}(X_{sil}-X_{s0l})$$
$$\left.+F_{3ts}\sum_{k=0}^{i}\sum_{l=0}^{j}\beta_{ik}\beta_{jl}X_{skl}\right\}$$
$$+Pu_{iq}u_{jr}\delta_{1t}+\sum_{c=0}^{m}\sum_{d=0}^{n}P_{cd}u_{ic}u_{jd}\delta_{1t}=0, \qquad (5)$$

where $\beta_{ik} = \alpha_{ik}/m$, $\beta_{jl} = \alpha_{jl}/n$, $\alpha_{ik} = 1-(\delta_{0k}+\delta_{ik})/2$, $\alpha_{jl} = 1-(\delta_{0l}+\delta_{jl})/2$, $t = 1 \sim 8$, $i = 1 \sim m$, $j = 1 \sim n$, $u_{iq} = u(\eta_i-\eta_q)$, $u_{jr} = u(\zeta_j-\zeta_r)$, $u_{ic} = u(\eta_i-\eta_c)$, $u_{jd} = u(\zeta_j-\zeta_d)$.

By retaining the quantities at main point (i,j) on the left hand side of the equation and putting other quantities on the right hand side, and using the matrix transition, the solution X_{pij} of the above equation (5) is obtained as follows:

$$\begin{aligned} X_{pij} = \sum_{t=1}^{8} & \left\{ \sum_{k=0}^{i} \beta_{ik} A_{pt} [X_{tk0} - X_{tkj}(1-\delta_{ik})] \right. \\ & + \sum_{l=0}^{j} \beta_{jl} B_{pt} [X_{t0l} - X_{til}(1-\delta_{jl})] \\ & \left. + \sum_{k=0}^{i} \sum_{l=0}^{j} \beta_{ik}\beta_{jl} C_{ptkl} X_{tkl} (1-\delta_{ik}\delta_{jl}) \right\} \\ & - A_{p1} P u_{iq} u_{jr} \\ & - \sum_{c=0}^{m} \sum_{d=0}^{n} P_{cd} u_{ic} u_{jd} \delta_{1t}, \end{aligned} \tag{6}$$

where $p = 1 \sim 8$, A_{pt}, B_{pt} and C_{ptkl} are given in Appendix A.

In the equation (6), the quantity X_{pij} is not only related to the quantities X_{tk0} and X_{t0l} at the boundary dependent points but also the quantities X_{tkj}, X_{til} and X_{tkl} at the inner dependent points. The number of unknown quantities is rather large. But with the spread of the area $[i,j]$ according to the pointed order, the quantities X_{tkj}, X_{til} and X_{tkl} at the inner dependent points can be eliminated and the equation (6) is rewritten as follows.

$$\begin{aligned} X_{pij} = & \sum_{d=1}^{6} \left\{ \sum_{f=0}^{i} a_{pijfd} X_{rf0} + \sum_{g=0}^{j} b_{pijgd} X_{s0g} \right\} \\ & + \overline{q}_{pij} P + \sum_{c=0}^{m} \sum_{d=0}^{n} \overline{q}_{pijcd} P_{cd}, \end{aligned} \tag{7}$$

where a_{pijfd}, b_{pijgd}, $\overline{q}_{pij}$ and $\overline{q}_{pijcd}$ are given in Appendix B.

The equation (7) gives the discrete solution of the fundamental differential equation (3) of the bending problem of a plate having a concentrated load and point supports, and the discrete Green function is chosen as $X_{8ij}a^2/[PD_0(1-\nu^2)]$, that is $w(x_0,y_0,x,y)/\overline{P}$.

The integral constants X_{rfo} and X_{sog} involved in the discrete solution (7) are all quantities at the discrete points along the edges $\zeta = 0$ $(y = 0)$ and $\eta = 0$ $(x = 0)$ of the rectangular plate. There are six integral constants at each discrete point. Half of them are self-evident according to the boundary conditions along the edges $\zeta = 0$ and $\eta = 0$ and half of them are needed to determine by the boundary conditions along the edges $\zeta = 1$ and $\eta = 1$.

Along the edge $\zeta = 0$ or $\zeta = 1$, $M_y = \theta_x = w = 0$ for simply supported boundary condition, $\theta_y = \theta_x = w = 0$ for clamped boundary condition, and $Q_y = M_{xy} = M_y = 0$ for free boundary condition. Along the edge $\eta = 0$ or $\eta = 1$, $M_x = \theta_y = w = 0$ for simply supported boundary condition, $\theta_y = \theta_x = w = 0$ for clamped boundary condition, $Q_x = M_{xy} = M_x = 0$ for free boundary condition.

4. Characteristic equation

By applying the Green function $w(x_0,y_0,x,y)/\overline{P}$ which is the displacement at a point (x_0,y_0) of a plate with a concentrated load $\overline{P}$ at a point (x,y) and omitting the effect of the rotary inertia, the displacement amplitude $\hat{w}(x_0,y_0)$ at a point (x_0,y_0) of the square plate during the free vibration is given as follows:

$$\hat{w}(x_0,y_0) = \int_0^b \int_0^a \rho h \omega^2 \hat{w}(x,y)[w(x_0,y_0,x,y)/\overline{P}]dxdy, \tag{8}$$

where ρ is the mass density of the plate material and ω is the circular frequency.

By using the numerical integration method and the following non-dimensional expressions,

$$\lambda^4 = \frac{\rho_0 h_0 \omega^2 a^4}{D_0(1-\nu^2)}, \quad \Lambda = 1/(\mu\lambda^4),$$

$$H(\eta,\zeta) = \frac{\rho(x,y)}{\rho_0}\frac{h(x,y)}{h_0}, W(\eta,\zeta) = \frac{\hat{w}(x,y)}{a},$$

$$G(\eta_0,\zeta_0,\eta,\zeta) = \frac{w(x_0,y_0,x,y)}{a}\frac{D_0(1-\nu^2)}{\overline{P}a},$$

where ρ_0 is the standard mass density , the characteristic equation is obtained from the equation (8) as

$$\begin{pmatrix} \mathbf{S_{00}} & \mathbf{S_{01}} & \mathbf{S_{02}} & \cdots & \mathbf{S_{0m}} \\ \mathbf{S_{10}} & \mathbf{S_{11}} & \mathbf{S_{12}} & \cdots & \mathbf{S_{1m}} \\ \mathbf{S_{20}} & \mathbf{S_{21}} & \mathbf{S_{22}} & \cdots & \mathbf{S_{2m}} \\ \vdots & \vdots & \vdots & \ddots & \vdots \\ \mathbf{S_{m0}} & \mathbf{S_{m1}} & \mathbf{S_{m2}} & \cdots & \mathbf{S_{mm}} \end{pmatrix} = 0 \tag{9}$$

where

$$\mathbf{S_{ij}} = \beta_{mj} \begin{bmatrix} \beta_{n0}H_{j0}G_{i0j0} - \Lambda\delta_{ij} & \cdots & \beta_{nn}H_{jn}G_{i0jn} \\ \beta_{n0}H_{j0}G_{i1j0} & \cdots & \beta_{nn}H_{jn}G_{i1jn} \\ \beta_{n0}H_{j0}G_{i2j0} & \cdots & \beta_{nn}H_{jn}G_{i2jn} \\ \vdots & \vdots & \vdots \\ \beta_{n0}H_{j0}G_{inj0} & \cdots & \beta_{nn}H_{jn}G_{injn} - \Lambda\delta_{ij} \end{bmatrix}.$$

The size of square matrix in the equation (9) is $(m+1)\times(n+1)$.

5. Numerical results

To investigate the validity of the proposed method, the frequency parameters are given for the rectangular plates with one or multiple point supports shown

Table 1 Convergence of natural frequency parameter λ for CCCC square plate with a central point support

	Mode sequence number				
$m \times n$	1st	2nd	3rd	4th	5th
6 × 6	10.017	10.017	12.241	12.812	16.283
8 × 8	9.412	9.412	10.902	11.479	13.815
10 × 10	9.165	9.165	10.218	11.164	12.963
12 × 12	9.039	9.039	9.875	11.000	12.555
14 × 14	8.966	8.966	9.675	10.905	12.325
16 × 16	8.919	8.919	9.545	10.844	12.182
18 × 18	8.888	8.888	9.455	10.803	12.086
Ex.*1416	8.766	8.766	9.121	10.645	11.714
Ex.1618	8.768	8.768	9.118	10.647	11.727
Ref. [7]	8.771	8.771	9.175	10.651	11.745

Ex.:The values obtained by using Richardson's extrapolation formula.

in Figure 1. The ratio of the standard thickness and length $h_0/a = 0.001$ is used. The Poisson's ratio $\nu = 0.3$ is adopted without any special indication. In all tables and figures, the symbols F, S, and C denote free, simply supported and clamped edges. Four symbols such as CFFF delegate the boundary conditions of the plate, the first indicating the conditions at $x = 0$, the second at $y = 0$, the third at $x = a$ and the fourth at $y = b$. All the convergent values of the frequency parameters are obtained for the plates by using Richardson's extrapolation formula for two cases of divisional numbers m (=n). Some of the results are compared with those reported previously.

5.1 Rectangular plates with a central point support

In order to examine the convergency, numerical calculation is carried out by varying the number of divisions m and n for a CCCC square plate with a central point support. The lowest 5 natural frequency parameters of the plate are shown in Table 1. It shows a good convergency of the numerical results by the present method. After studying these results, it is decided to obtain the convergent results of frequency parameter by using Richardson's extrapolation formula for two cases of divisional numbers m (=n) of 14 and 16. By the same method, the suitable number of divisions m(= n) can be determined for the other plates.

Tables 2∼ 4 show the numerical values for the lowest 4 natural frequency parameter λ of rectan-

Table 2 Natural frequency parameter λ for SSSS rectangular plates with a central point support

		Mode sequence number			
μ	$m \times n$	1st	2nd	3rd	4th
0.5	14 × 14	9.195	10.132	13.479	15.242
	16 × 16	9.172	10.055	13.427	15.027
	Ex.	9.096	9.802	13.259	14.325
1.0	14 × 14	7.297	7.297	7.828	9.254
	16 × 16	7.272	7.272	7.743	9.216
	Ex.	7.191	7.191	7.466	9.095
	Ref. [7]	7.192	7.192	7.466	9.098
2.0	14 × 14	4.598	5.066	6.740	7.621
	16 × 16	4.586	5.027	6.714	7.514
	Ex.	4.548	4.901	6.629	7.162

Table 3 Natural frequency parameter λ for CCCC rectangular plates with a central point support

		Mode sequence number			
μ	$m \times n$	1st	2nd	3rd	4th
0.5	14 × 14	11.712	12.636	16.804	17.458
	16 × 16	11.674	12.534	16.702	17.160
	Ex.	11.549	12.200	16.368	16.185
1.0	14 × 14	8.966	8.966	9.675	10.905
	16 × 16	8.919	8.919	9.545	10.844
	Ex.	8.766	8.766	9.121	10.645
	Ref. [7]	8.771	8.771	9.175	10.651
2.0	14 × 14	5.856	6.318	8.402	8.729
	16 × 16	5.837	6.267	8.351	8.580
	Ex.	5.774	6.100	8.184	8.093

Table 4 Natural frequency parameter λ for CFFF rectangular plates with a central point support

		Mode sequence number			
μ	$m \times n$	1st	2nd	3rd	4th
0.5	14 × 14	3.215	3.946	7.163	7.896
	16 × 16	3.206	3.944	7.149	7.847
	Ex.	3.176	3.938	7.105	7.689
1.0	14 × 14	2.992	3.028	4.986	5.746
	16 × 16	2.990	3.024	4.984	5.735
	Ex.	2.983	3.009	4.980	5.700
2.0	14 × 14	2.372	2.454	3.790	4.570
	16 × 16	2.371	2.452	3.779	4.547
	Ex.	2.368	2.447	3.744	4.469

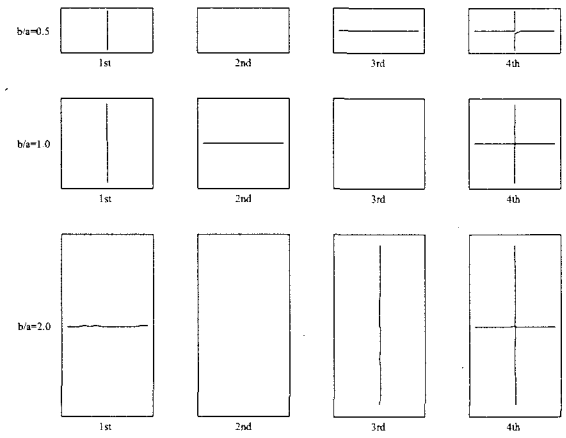

Fig. 3 Nodal patterns for SSSS rectangular plates with a central point support.

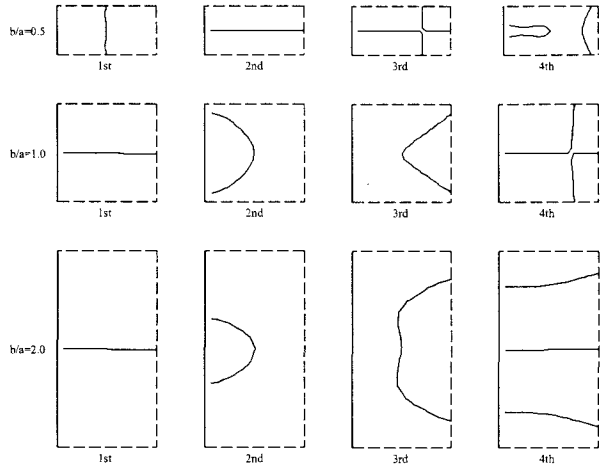

Fig. 4 Nodal patterns for CFFF rectangular plates with a central point support.

gular plates with a central point support. Three kinds of boundary conditions and the aspect ratios $\mu = 0.5, 1.0, 2.0$ are considered. The results obtained by Kim and Dickinson [7] are also shown in the table. It can be noted the present results agree well with those of Kim and Dickinson and the frequency parameters increase with the increase of the constraint of the boundary conditions. The nodal lines of 4 modes of free vibration of SSSS plates with $\mu = 0.5, 1.0, 2.0$ are shown in Figure 3. It can be observed for the modes with nodal lines passing through the center of the plate, the frequency parameters and mode shapes are the same for the plates with or without a central point support. The mode with no nodal line is the third one for the square plate, but the second mode for plates with $\mu = 0.5, 2.0$. The same phenomenon can also be found in the modes of CCCC plates which are similar to the modes of SSSS plates except that

Table 5 Natural frequency parameter λ for CFFF square plates with multiple point supports

Fig.5	Refs.	Mode sequence number ($\nu = 0.333$) 1st	2nd	3rd	4th
(*I*)	Present	2.570	4.154	5.205	6.451
	Ref.[4]	2.525	4.099	5.162	6.364
	Ref.[7]	2.538	4.127	5.166	6.420
(*II*)	Present	3.938	4.343	5.294	6.831
	Ref.[4]	3.891	4.263	5.322	6.749
	Ref.[7]	3.896	4.270	5.322	6.763
(*III*)	Present	4.811	6.115	6.249	7.260
	Ref.[7]	4.753	6.023	6.147	7.189
(*IV*)	Present	3.225	4.118	5.184	7.054
	Ref.[5]	3.173	4.086	5.228	6.999
		Mode sequence number ($\nu = 0.3$)			
		1st	2nd	3rd	4th
(*I*)	Present	2.586	4.173	5.166	6.467
	Ref.[7]	2.562	4.172	5.158	6.473
(*II*)	Present	3.958	4.349	5.373	6.837
	Ref.[7]	3.912	4.310	5.338	6.807
(*III*)	Present	4.807	6.062	6.272	7.238
	Ref.[7]	4.744	6.081	6.204	7.201
(*IV*)	Present	3.133	4.221	5.280	6.831
(*V*)	Present	3.154	4.288	6.141	8.002
(*VI*)	Present	6.048	6.358	6.698	8.267

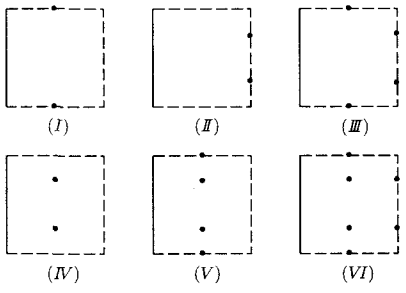

Fig. 5 CFFF square plates with multiple point supports.

there is a change of mode order in the 3rd and 4th modes for $\mu = 0.5, 2.0$. The nodal lines of 4 modes of free vibration of CFFF plates with $\mu = 0.5, 1.0, 2.0$ are shown in Figure 4.

5.2 Rectangular plates with multiple point supports

Table 5 presents the numerical values of CFFF plates (shown in Figure 5) for the lowest 4 natu-

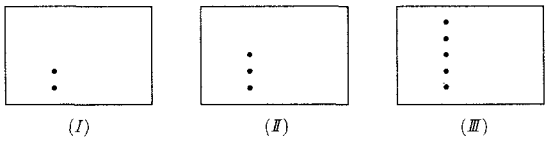

Fig. 6 SSSS rectangular plates with multiple point supports.

ral frequency parameter. In Figure 5, CFFF square plates have multiple point supports located (I) at points $(a/2, 0)$ and $(a/2, b)$, or (II) at points $(a, b/4)$ and $(a, 3b/4)$, or (III) at points $(a/2, 0)$, $(a/2, b)$, $(a, b/4)$ and $(a, 3b/4)$, or (IV) at points $(a/2, b/4)$ and $(a/2, 3b/4)$, or (V) at points $(a/2, 0)$, $(a/2, b)$, $(a/2, b/4)$ and $(a/2, 3b/4)$, or (VI) at points $(a/2, 0)$, $(a/2, b)$, $(a/2, b/4)$, $(a/2, 3b/4)$, $(a, b/4)$ and $(a, 3b/4)$. The first three cases in Figure 5 show the plates with the point supports along the edges. Figure 5 (IV) shows the plate with interior point supports. Figure 5 (V) and (VI) are the combination of Figure 5 (I), (IV) and Figure 5 (III), (IV), respectively. In order to compare the present results with those obtained by Saliba [4,5] and Kim and Dickinson [7], two kinds of Poisson's ratio $\nu = 0.333$ and $\nu = 0.3$ are used. It can be noted the present results are in good agreement with the comparison results and the frequency parameters increase with the increase of the number of point supports. By comparing the results of the plates shown in Figure 5 (I), (II) and (IV), it can be seen the best positions of the two point support are at points $(a, b/4)$ and $(a, 3b/4)$.

Figure 6 shows the SSSS rectangular plates with multiple point supports located at (I) points $(c, b/6)$ and $(c, b/3)$, or (II) points $(c, b/6)$, $(c, b/3)$ and $(c, b/2)$, or (III) points $(c, b/6)$, $(c, b/3)$, $(c, b/2)$, $(c, 2b/3)$ and $(c, 5b/6)$. The numerical values for the lowest 4 natural frequency parameter λ of these plates are presented in Table 6. It can be seen the frequency parameters increase with the increase of the number of point supports. The results of an SSSS plate with a mid-line support at $x = a/2$ obtained by Xiang and Wei are also presented in Table 6 for $h_0/a = 0.01$. It can be seen for the specific ratio μ and the case of point support, the fundamental frequency parameter increase with the increase of the value of c, and all the frequency parameters increase when the number of point supports increases. It can also be seen with the increase of the number of point supports, the frequency parameters of square plates with multiple point supports are closer to those obtained by Xiang and Wei [9] for an SSSS plate with a line support.

Table 6 Natural frequency parameter λ for SSSS rectangular plates with mutiple point supports

μ	c	Fig.6	Mode sequence number 1st	2nd	3rd	4th
1.0	$a/6$	(I)	5.131	7.240	8.089	9.633
		(II)	5.358	7.450	8.509	9.671
		(III)	5.446	7.669	8.845	10.362
	$a/3$	(I)	5.692	7.274	8.567	10.157
		(II)	6.123	7.784	9.014	10.157
		(III)	6.240	8.262	10.157	10.891
	$a/2$	(I)	6.124	7.191	9.029	9.095
		(II)	7.191	7.379	9.094	9.095
		(III)	7.191	8.516	9.095	9.944
		Ref. [9]	7.189	8.517	9.091	9.946
1.5	$a/6$	(I)	4.368	5.748	7.205	7.342
		(II)	4.735	5.765	7.314	7.852
		(III)	4.966	6.072	7.650	8.532
	$a/3$	(I)	4.643	6.231	7.325	7.532
		(II)	5.319	6.233	7.459	8.350
		(III)	5.810	6.802	8.242	9.870
	$a/2$	(I)	4.758	6.779	7.282	7.729
		(II)	5.644	6.779	7.729	8.356
		(III)	6.779	7.729	8.226	8.854
2.0	$a/6$	(I)	3.971	5.116	6.013	6.862
		(II)	4.347	5.134	6.206	7.207
		(III)	4.788	5.426	6.406	7.589
	$a/3$	(I)	4.096	5.653	6.296	6.912
		(II)	4.634	5.830	6.684	7.336
		(III)	5.652	6.224	7.101	8.169
	$a/2$	(I)	4.140	5.934	6.629	7.190
		(II)	4.743	6.629	7.190	7.257
		(III)	6.629	7.190	8.035	8.093

Figure 7 presents the changes of the first three frequency parameters with the aspect ratio μ for SSSS rectangular plates shown in Figure 6 (III). It can be noted with the increase of the aspect ratio μ, all the frequency parameters decrease. The trend of the change in the plates with point supports are the same as those in the plates without point support.

6. Conclusions

A discrete method is extended for analyzing the free vibration problem of rectangular plates with one or multiple point supports. The concentrated loads with Dirac's delta functions are used to simulate the point

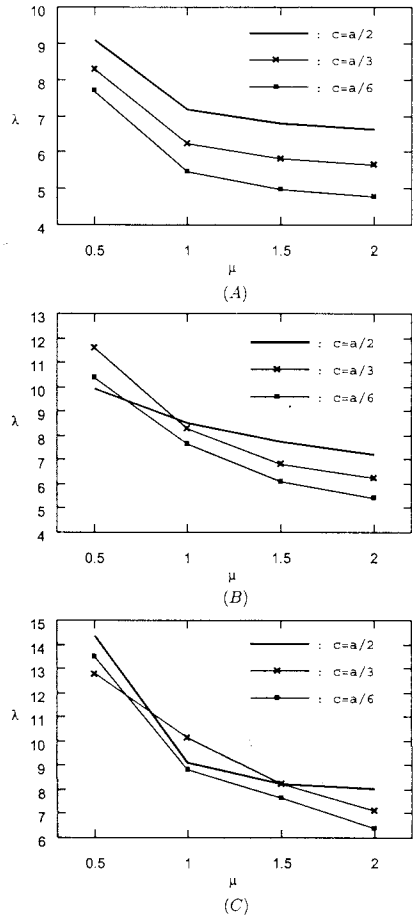

Fig. 7 Frequency parameter λ of SSSS rectangular plates versus the aspect ratio μ. (A) the fist frequency parameter; (B) the second frequency parameter; (C) the third frequency parameter.

supports which limit the displacements of the plate but don't offer constraint on the slopes. The fundamental differential equations of a plate with point supports involving Dirac'delta functions are established and satisfied exactly throughout the whole plate. The characteristic equation of the free vibration is obtained by using the Green function. The effects of the number and position of point supports on the frequencies are considered. The results by the present method have been compared with those previously reported. It shows that the present results have a good convergence and satisfactory accuracy.

REFERENCES

1) A.V.BAPAT, N.VENKATRAMANI and S.SURYANARAYAN 1988 *Journal of Sound and Vibration* **120**, 107-125. A new approach for the representation of a point support in the analysis of plates.

2) A.V.BAPAT, N.VENKATRAMANI and S.SURYANARAYAN 1988 *Journal of Sound and Vibration* **124**, 555-576. The use of flexibility functions with negative domains in the vibration analysis of asymmetrically point-supported rectangular plates.

3) A.V.BAPAT and S.SURYANARAYAN 1989 *Journal of Sound and Vibration* **134**, 291-313. Free vibrations of rectangular plates with interior point supports.

4) H.T.SALIBA 1984 *Journal of Sound and Vibration* **94**, 381-395. Free vibration analysis of rectangular cantilever plates with symmetrically distributed point supports along the edges.

5) H.T.SALIBA 1988 *Journal of Sound and Vibration* **127**, 77-89. Free vibration analysis of rectangular cantilever plates with symmetrically distributed lateral point supports.

6) M.-H.HUANG and D.P.THAMBIRATNAM 2001 *Journal of Engineering Mechanics* **240**, 567-580. Free vibration analysis of rectangular plates on elastic intermediate supports.

7) C.S.KIM and S.M.DICKINSON 1987 *Journal of Sound and Vibration* **117**, 249-261. The flexural vibration of rectangular plates with point supports.

8) Y.B.ZHAO, G.W.WEI and Y.XIANG 2002 *International Journal of Solids and Structures* **39**, 1361-1383. Plate vibration under irregular internal supports.

9) Y.XIANG and G.W.WEI 2002 *Journal of Sound and Acoustics* **124**, 545-551. Exact solutions for vibration of multi-span rectangular Mindlin plates.

10) M.HUANG, X.Q.MA, T.SAKIYAMA, H.MATSUDA and C.MORITA 2004 *Journal of Sound and Vibration* Free vibration analysis of rectangular plates with variable thickness and point supports. Submitted.

11) M.HUANG, X.Q.MA, T.SAKIYAMA, H.MATSUDA and C.MORITA 2004 *Journal of Applied Mechanics* **Vol.7**, 225-232. Free vibration analysis of square plates resting on non-homogeneous elastic foundation.

12) M.HUANG, X.Q.MA, T.SAKIYAMA, H.MATSUDA and C.MORITA 2003 *Journal of Applied Mechanics* **Vol.6**, 331-340. A discrete method for bending and free vibration analysis of orthotropic plates with non-uniform thickness.

13) M.HUANG, X.Q.MA, T.SAKIYAMA, H.MATSUDA and C.MORITA 2002 *Journal of Applied Mechanics*

Vol.5, 151-160. Free vibration analysis of simply supported orthotropic square plates with a square hole.

Appendix A

$A_{p1}=\gamma_{p1}$, $A_{p2}=0$,$A_{p3}=\gamma_{p2}$, $A_{p4}=\gamma_{p3}$, $A_{p5}=0$, $A_{p6}=\gamma_{p4}+\nu\gamma_{p5}$, $A_{p7}=\gamma_{p6}$, $A_{p8}=\gamma_{p7}$, $B_{p1}=0$, $B_{p2}=\mu\gamma_{p1}$, $B_{p3}=\mu\gamma_{p3}$, $B_{p4}=0$, $B_{p5}=\mu\gamma_{p2}$, $B_{p6}=\mu\gamma_{p6}$, $B_{p7}=\mu(\nu\gamma_{p1}+\gamma_{p5})$, $B_{p8}=\gamma_{p8}$, $C_{p1kl}=\mu(\gamma_{p3}+k_{kl}\gamma_{p7})$, $C_{p2kl}=\mu\gamma_{p2}+k_{kl}\gamma_{p8}$, $C_{p3kl}=J\gamma_{p6}$, $C_{p4kl}=I_{kl}\gamma_{p4}$, $C_{p5kl}=I_{kl}\gamma_{p5}$, $C_{p6kl}=-\mu\gamma_{p7}$, $C_{p7kl}=-\gamma_{p8}$, $C_{p8kl}=0$, $[\gamma_{pk}]=[\overline{\gamma}_{pk}]^{-1}$, $\overline{\gamma}_{11}=\beta_{ii}$, $\overline{\gamma}_{12}=\mu\beta_{jj}$, $\overline{\gamma}_{22}=-\mu\beta_{ij}$, $\overline{\gamma}_{23}=\beta_{ii}$, $\overline{\gamma}_{25}=\mu\beta_{jj}$, $\overline{\gamma}_{31}=-\mu\beta_{ij}$, $\overline{\gamma}_{33}=\mu\beta_{jj}$, $\overline{\gamma}_{34}=\beta_{ii}$, $\overline{\gamma}_{44}=-I_{ij}\beta_{ij}$, $\overline{\gamma}_{46}=\beta_{ii}$, $\overline{\gamma}_{47}=\mu\nu\beta_{jj}$, $\overline{\gamma}_{55}=-I_{ij}\beta_{ij}$, $\overline{\gamma}_{56}=\nu\beta_{ii}$, $\overline{\gamma}_{57}=\mu\beta_{jj}$, $\overline{\gamma}_{63}=-J_{ij}\beta_{ii}$, $\overline{\gamma}_{66}=\mu\beta_{jj}$, $\overline{\gamma}_{67}=\beta_{ii}$, $\overline{\gamma}_{71}=-\mu k_{ij}\beta_{ij}$, $\overline{\gamma}_{76}=\mu\beta_{ij}$, $\overline{\gamma}_{78}=\beta_{ii}$, $\overline{\gamma}_{82}=-H_{ij}\beta_{ij}$, $\overline{\gamma}_{87}=\beta_{ij}$, $\overline{\gamma}_{88}=\beta_{jj}$, other $\overline{\gamma}_{pk}=0$, $\beta_{ij}=\beta_{ii}\beta_{jj}$

Appendix B

$a_{1i0i1}=a_{3i0i2}=a_{4i0i3}=1, a_{6i0i4}=a_{7i0i5}=a_{8i0i6}=1$

$b_{20jj1}=b_{30jj2}=b_{50jj3}=1, b_{60jj4}=b_{70jj5}=b_{80jj6}=1,$

$$a_{pijfd}=\sum_{t=1}^{8}\Bigg\{\sum_{k=0}^{i}\beta_{ik}A_{pt}[a_{tk0fd}-a_{tkjfd}(1-\delta_{ki})]+\sum_{l=0}^{j}\beta_{jl}B_{pt}[a_{t0lfd}-a_{tilfd}(1-\delta_{lj})]+\sum_{k=0}^{i}\sum_{l=0}^{j}\beta_{ik}\beta_{jl}C_{ptkl}a_{tklfd}(1-\delta_{ki}\delta_{lj})\Bigg\}$$

$$b_{pijfd}=\sum_{t=1}^{8}\Bigg\{\sum_{k=0}^{i}\beta_{ik}A_{pt}[b_{tk0gd}-b_{tkjgd}(1-\delta_{ki})]+\sum_{l=0}^{j}\beta_{jl}B_{pt}[b_{t0lgd}-b_{tilgd}(1-\delta_{lj})]+\sum_{k=0}^{i}\sum_{l=0}^{j}\beta_{ik}\beta_{jl}C_{ptkl}b_{tklgd}(1-\delta_{ki}\delta_{lj})\Bigg\}$$

$$\overline{q}_{pij}=\sum_{t=1}^{8}\Bigg\{\sum_{k=0}^{i}\beta_{ik}A_{pt}[\overline{q}_{tk0}-\overline{q}_{tkj}(1-\delta_{ki})]+\sum_{l=0}^{j}\beta_{jl}B_{pt}[\overline{q}_{t0l}-\overline{q}_{til}(1-\delta_{lj})]+\sum_{k=0}^{i}\sum_{l=0}^{j}\beta_{ik}\beta_{jl}C_{ptkl}-A_{p1}u_{iq}u_{jr}$$

$$\overline{q}_{fpijcd}=\sum_{e=1}^{8}\Bigg\{\sum_{k=0}^{i}\beta_{ik}A_{pe}[\overline{q}_{fek0cd}-\overline{q}_{fekjcd}(1-\delta_{ki})]+\sum_{l=0}^{j}\beta_{jl}B_{pe}[\overline{q}_{fe0lcd}-\overline{q}_{feilcd}(1-\delta_{lj})]+\sum_{k=0}^{i}\sum_{l=0}^{j}\beta_{ik}\beta_{jl}C_{pekl}\overline{q}_{feklcd}(1-\delta_{ki}\delta_{lj})\Bigg\}$$

$$-\gamma_{pf}u_{ik}u_{jr}\overline{u}_{fkl}$$

(Received April 15 2005)